THE JOURNAL OF BIOLOGICAL CHEMISTRY VOL. 288, NO. 40, pp. 28783–28791, October 4, 2013

Histone Deacetylase Inhibition Promotes Osteoblast Maturation by Altering the Histone H4 Epigenome and Reduces Akt Phosphorylation*

Received for publication, May 29, 2013, and in revised form, July 26, 2013 Published, JBC Papers in Press, August 12, 2013, DOI 10.1074/jbc.M113.489732

Amel Dudakovic[‡], Jared M. Evans[§], Ying Li[§], Sumit Middha[§], Meghan E. McGee-Lawrence[‡], Andre J. van Wijnen[‡¶], and Jennifer J. Westendorf[‡¶1]

From the [‡]Department of Orthopedic Surgery, [§]Division of Biomedical Statistics and Informatics, and [¶]Center of Regenerative Medicine, Mayo Clinic, Rochester, Minnesota 55905

Background: Histone deacetylase (HDAC) inhibition promotes bone formation *in vitro* via undefined epigenetic events.
Results: Microarray and ChIP-Seq analyses revealed genomic areas where H4 acetylation is altered by HDAC inhibitors and identified differentially regulated genes.
Conclusion: Suberoylanilide hydroxamic acid increases H4 acetylation and suppresses phosphorylation of insulin/Akt signaling mediators in osteoblasts.
Significance: Epigenetic profiling is a powerful means to gain mechanistic insights into bone anabolic processes.

Bone has remarkable regenerative capacity, but this ability diminishes during aging. Histone deacetylase inhibitors (HDIs) promote terminal osteoblast differentiation and extracellular matrix production in culture. The epigenetic events altered by HDIs in osteoblasts may hold clues for the development of new anabolic treatments for osteoporosis and other conditions of low bone mass. To assess how HDIs affect the epigenome of committed osteoblasts, MC3T3 cells were treated with suberoylanilide hydroxamic acid (SAHA) and subjected to microarray gene expression profiling and high-throughput ChIP-Seq analysis. As expected, SAHA induced differentiation and matrix calcification of osteoblasts *in vitro*. ChIP-Seq analysis revealed that SAHA increased histone H4 acetylation genome-wide and in differentially regulated genes, except for the 500 bp upstream of transcriptional start sites. Pathway analysis indicated that SAHA increased the expression of insulin signaling modulators, including *Slc9a3r1*. SAHA decreased phosphorylation of insulin receptor β, Akt, and the Akt substrate FoxO1, resulting in FoxO1 stabilization. Thus, SAHA induces genome-wide H4 acetylation and modulates the insulin/Akt/FoxO1 signaling axis, whereas it promotes terminal osteoblast differentiation *in vitro*.

Epigenetics is defined as heritable changes in gene expression that are not linked to changes in DNA sequence. Epigenetic events can be transferred to future generations via meiotic inheritance or to somatic daughter cells via mitotic inheritance. Epigenetic signatures are sensitive to environmental cues, and a greater understanding of epigenetic events in osteoblasts could improve bone tissue-engineering strategies and identify novel anabolic targets. The major epigenetic mechanisms affecting gene expression are post-translational modifications of histones, methylation of genomic DNA, and activities of noncoding RNAs (1). Histone acetylation is controlled by histone acetyltransferases and histone deacetylases (HDACs),[2] which add or remove acetyl groups to lysine side chains, respectively. The addition of acetyl groups to histones relaxes chromatin and promotes the recruitment of transcriptional cofactors, whereas HDACs remove acetyl groups from histones to compact the chromatin structure (2, 3). Histone acetylation is generally associated with transcriptional activation, whereas deacetylation of histones represses gene expression.

Compounds that inhibit HDACs to increase acetylation of histones and induce gene expression have gained attention as clinical therapeutics. Such histone deacetylase inhibitors (HDIs), including suberoylanilide hydroxamic acid (SAHA; vorinostat, Zolinza™), are used worldwide as treatments for epilepsy, cancer, and other conditions (4, 5). The utility of these and other HDIs for a broader range of diseases, such as HIV and cystic fibrosis, is under investigation (6, 7).

Skeletal development and bone mass maintenance are dynamic and complex processes that require precise control of transcriptional events in multiple cells types and are sensitive to changes in HDAC levels (8). HDIs interfere with osteoclast survival and function *in vitro* (9, 10) but promote osteoblast terminal differentiation *in vitro*. HDIs accelerate matrix production and induce the expression of osteoblast genes in osteogenic cell lines, primary calvarial cells, calvarial organ cultures, and mesenchymal progenitor cells (11–14). HDIs promote osteoblast differentiation at the expense of adipocyte differentiation *in*

* This work was supported, in whole or in part, by National Institutes of Health Grants R01 AR048147 and R01 DE020194 (to J. J. W.), Grant AR049069 (to A. J. v. W.), and Grant AR60140 (to M. E. M.-L.). This work was also supported by the Mayo Clinic Center for Individualized Medicine.
ChIP-Seq and microarray data were deposited in the Gene Expression Omnibus (GEO) Database with accession number GSE50552.
[1] To whom correspondence should be addressed: Depts. of Orthopedic Surgery and Biochemistry and Molecular Biology, Mayo Clinic, 200 First St. SW, Rochester, MN 55905. Tel.: 507-538-5651; Fax: 507-284-5075; E-mail: westendorf.jennifer@mayo.edu.

[2] The abbreviations used are: HDAC, histone deacetylase; HDI, histone deacetylase inhibitor; SAHA, suberoylanilide hydroxamic acid; DMSO, dimethyl sulfoxide; qPCR, real-time quantitative PCR; TSS, transcriptional start site.

vitro (15). These positive effects of HDIs on *in vitro* osteoblast maturation are due at least in part to their ability to promote the activity of Runx2, a key osteoblastogenesis transcription factor that binds several HDACs (16–19).

We previously reported that HDIs promote osteoblast differentiation of MC3T3-E1 osteoblasts, primary osteoblasts, and *ex vivo* calvarial cultures (12) and differentially regulate expression of numerous genes in osteoblasts (20). In this study, we investigated the epigenetic events that promote osteoblast differentiation *in vitro* after exposure to the HDI SAHA. ChIP with massively parallel high-throughput sequencing (ChIP-Seq) was used to map genome-wide histone H4 acetylation in the presence or absence of SAHA. These data were compared with microarray gene expression results. SAHA generally increased H4 hyperacetylation in highly induced genes compared with suppressed genes. Pathway analysis of the expression profile and genome-wide H4 acetylation indicated that SAHA stimulated the expression of key insulin signaling pathway inhibitors and reduced activation and phosphorylation of insulin signaling mediators. Thus, HDIs promoted terminal osteoblast differentiation despite reductions in insulin receptor and Akt kinase activity. This study demonstrates the utility of epigenetic profiling to advance the mechanistic understanding of bone anabolic processes.

EXPERIMENTAL PROCEDURES

Cell Culture—MC3T3 sc4 murine calvarial osteoblasts (21) were purchased from American Type Culture Collection and maintained in maintenance medium (α-minimal essential medium without ascorbic acid (Invitrogen) containing 10% FBS (Invitrogen), 100 units/ml penicillin, and 100 μg/ml streptomycin (cellgro®)).

Osteoblast Mineralization Assay—MC3T3 sc4 cells were plated in 6-well plates in maintenance medium. At confluence, maintenance medium was replaced with osteogenic medium (α-minimal essential medium supplemented with 50 μg/ml ascorbic acid (Sigma) and 4 mM β-glycerol phosphate (Sigma)). SAHA and/or its solvent dimethyl sulfoxide (DMSO) was added at day 4, and cultures were continued for 3 more days. On day 7, the medium was aspirated, cells were washed once with PBS, and fresh osteogenic medium was added. The medium was changed every 2–3 days. On day 26, cells were fixed in 10% neutral buffered formalin and stained with 2% Alizarin red. For insulin studies, MC3T3 sc4 osteoblasts were treated with SAHA (10 μM) and/or insulin (100 nM) from days 4 though 7.

Western Blotting—MC3T3 sc4 cells were plated in maintenance medium on 10-cm dishes until they reached 60% confluence. Cells were then treated with SAHA or vehicle (DMSO). Cells were lysed in radioimmunoprecipitation buffer (150 mM NaCl, 50 mM Tris (pH 7.4), 1% sodium deoxycholate, 0.1% SDS, and 1% Triton X-100) supplemented with protease inhibitor mixture (Sigma) and PMSF (Sigma). Lysates were cleared by centrifugation. Protein concentrations were determined using the *DC*™ protein assay (Bio-Rad). Proteins were resolved by SDS-PAGE and transferred to polyvinylidene difluoride membranes. After blocking in 5% nonfat dry milk for 45 min at room temperature, primary antibodies were added overnight at 4 °C, followed by secondary antibodies for 1 h at room temperature. Proteins were visualized using an ECL$^+$ detection kit. Primary antibodies used were anti-actin (1:10,000; Santa Cruz Biotechnology sc-1616), anti-acetylated H3 (Lys^9/Lys^{14}; 1:10,000; Millipore 06-599), anti-H3 (1:20,000; Millipore 05-928), anti-tetra-acetylated H4 (Lys^5/Lys^8/Lys^{12}/Lys^{16}; 1:20,000; Millipore 06-866), anti-phospho-insulin receptor β (Tyr^{1146}/Tyr^{1150}/Tyr^{1151}; 1:1000; Cell Signaling 3024), anti-insulin receptor β (1:1000; Cell Signaling 3025), anti-phospho-Akt (Ser^{473}; 1:4000; R&D Biosystems AF887), anti-Akt (1:10,000; Cell Signaling 9272), anti-phospho-FoxO1 (Thr^{24}; 1:2000; Cell Signaling 2599), anti-FoxO1 (1:2000; Cell Signaling 2880), and anti-Nherf1 (1:1000; Abcam Ab3452). Phosphorylated protein antibodies were removed with Restore Western blot stripping buffer (Pierce), and membranes were reblotted with antibodies that recognize the relevant proteins irrespective of phosphorylation. Western blot quantification was performed with ImageJ software.

ChIP-Seq Analysis—MC3T3 sc4 cells were differentiated in 10-cm dishes in osteogenic medium for 4 days. On day 4, SAHA or vehicle was added to the differentiating cells. Two hours later, the medium was removed, and cells were washed twice with PBS. Collagenase digests were performed with 1 mg/ml type II collagenase (Worthington) and 1 mg/ml BSA (Sigma) in Hanks' balanced salt solution for 40 min (cells were exposed to SAHA or vehicle during this incubation). After collagenase digestion, cells were harvested by scraping and washed three times with PBS supplemented with protease inhibitor mixture. Cells were cross-linked with 1% formaldehyde for 15 min at room temperature. Cells were washed three times with PBS supplemented with protease inhibitor mixture and lysed (50 mM Tris-HCl (pH 8.0), 1% SDS, and 10 mM EDTA). This ChIP solution was sonicated to generate 200–500-bp DNA fragments, diluted (16.7 mM Tris-HCl (pH 8.0), 0.01% SDS, 1.1% Triton X-100, 1.2 mM EDTA, and 167 mM NaCl), and precleared with Dynabeads Protein G magnetic beads (Invitrogen) for 1 h. Immunoprecipitations were performed with 10 μg of antibodies overnight at 4 °C. Anti-tetraacetylated H4 (Lys^5/Lys^8/Lys^{12}/Lys^{16}; Millipore 06-866) and IgG (Vector Labs I-1000) antibodies were used. Dynabeads were added and incubated for 1 h. Immune complexes and beads were washed with low-salt buffer (20 mM Tris-HCl (pH 8.0), 0.1% SDS, 1% Triton X-100, 2 mM EDTA, and 150 mM NaCl), high-salt buffer (20 mM Tris-HCl (pH 8.0), 0.1% SDS, 1% Triton X-100, 2 mM EDTA, and 500 mM NaCl), LiCl buffer (10 mM Tris-HCl (pH 8.0), 250 mM LiCl, 1% Nonidet P-40, 1% sodium deoxycholate, and 1 mM EDTA), and 10 mM Tris-HCl (pH 8.0) and 1 mM EDTA. Immunoprecipitations were eluted (1% SDS and 100 mM $NaHCO_3$) twice, and elutes were combined. Heating samples to 65 °C reversed cross-linking, and proteins were digested with proteinase K. DNA was extracted with phenol/chloroform/isoamyl alcohol (25:24:1, v/v; Invitrogen), precipitated with ethanol, and reconstituted with 50 μl of water. Sequencing libraries were prepared, and massively parallel high-throughput sequencing was performed on an Illumina HiSeq 2000 system. The 50-bp reads were aligned to the reference genome using the Burrows-Wheeler transform, and a minimum mapping quality filter of 20 was applied (22). Enriched regions were identified and analyzed with MACS v1.4.0 (model-based analysis for ChIP-Seq)

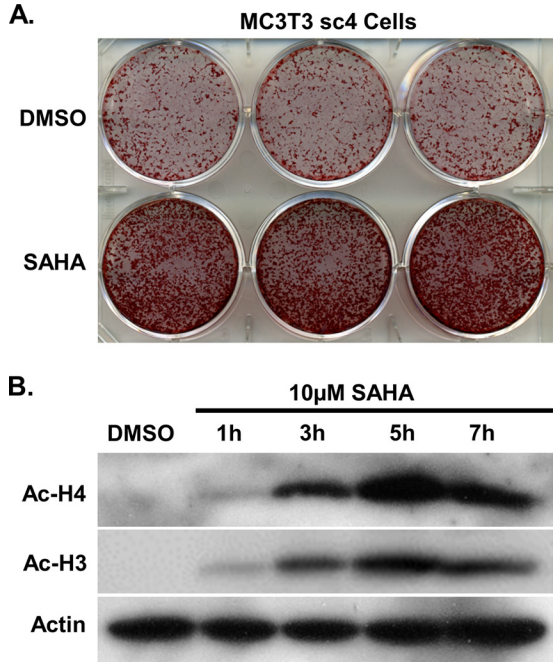

FIGURE 1. **SAHA enhances osteoblast differentiation and induces H3 and H4 acetylation.** *A*, Alizarin red stain of MC3T3 sc4 cells in osteogenic medium for 26 days. DMSO and SAHA (10 μM) were added on day 4 and removed on day 7 of differentiation (triplicates are shown). *B*, Western blots showing time-dependent induction of H3 and H4 acetylation (*Ac*) in the presence of SAHA. MC3T3 sc4 cells were exposed to osteogenic medium for 4 days and then treated with DMSO or SAHA (10 μM) as shown.

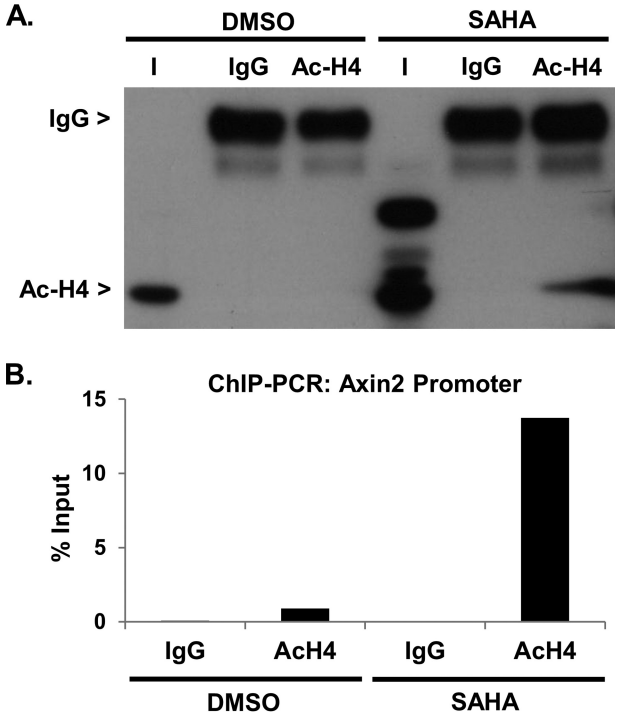

FIGURE 2. **SAHA induces global chromatin H4 acetylation and enhances H4 acetylation on the *Axin2* promoter.** MC3T3 sc4 cells were differentiated in osteogenic medium for 4 days and treated with DMSO or SAHA (20 μM) for 2 h before the ChIP assay was performed with anti-acetylated H4 and IgG antibodies. *A*, Western blot from ChIP assay showing successful pulldown of acetylated H4 (*Ac-H4*) in the presence of SAHA. *B*, ChIP-PCR showing H4 acetylation of the *Axin2* promoter with and without SAHA ($n = 2$). Data are normalized to input DNA.

(23) and CEAS v1.0.2 (*cis*-regulatory element annotation system) (24, 25).

ChIP-PCR Analysis—DNA isolated during ChIP assays was subjected to real-time PCR analysis using primers for the *Axin2* promoter (5′-TTATGGGAACACGCTTCCTC-3′ and 5′-ATGTACCTGGGTTTCCTTGC-3′) and iQ SYBR Green Supermix (Bio-Rad). Threshold values were normalized to input DNA.

Gene Expression Analysis Using Microarrays—MC3T3 sc4 cells were cultured in 10-cm dishes and differentiated in osteogenic medium for 4 days in the presence of DMSO or SAHA as described above for ChIP-Seq. RNA was isolated with the RNeasy Plus kit (Qiagen). Microarray experiments were performed on the Illumina MouseWG-6 v2.0 R3 array. GenomeStudio (Illumina) was used to export the data (no background substitution or normalization). Fastlo was used for normalization, $\log_2$ conversion, and noise filtering of the data (26). Four samples were included for each condition. Differential gene expression between the DMSO and SAHA treatment groups was analyzed with a paired *t* test.

Quantitative Real-time PCR (qPCR)—RNA was isolated using the RNeasy Plus kit and reverse-transcribed into cDNA using the SuperScript III first-strand synthesis system (Invitrogen). Gene expression was measured by qPCR. Reactions included 37.5 ng of cDNA/15 μl with iQ SYBR Green Supermix and the MyiQ single color real-time PCR detection system. Transcript levels were normalized to the housekeeping gene *Gapdh*. Gene expression levels were quantified using the $2^{\Delta\Delta Ct}$ method. Gene-specific primer sequences were as follows: *Gapdh*, 5′-GGGAAGCCCATCACCATCTT (forward) and 5′-GCCTCACCCCATTTGATGTT (reverse); and *Slc9a3r1*, 5′-CAGCACG-

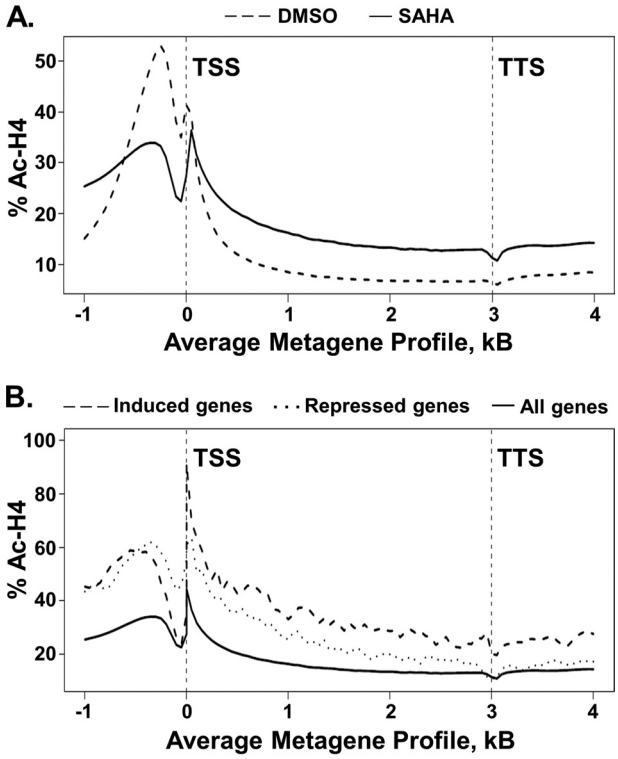

FIGURE 3. **SAHA induces genome-wide H4 acetylation.** MC3T3 sc4 cells were differentiated in osteogenic medium for 4 days and treated with DMSO or SAHA (20 μM) for 2 h before ChIP-Seq was performed with anti-acetylated H4 (*Ac-H4*) and IgG antibodies. *TTS*, transcriptional termination site. *A*, average ChIP-Seq profiles of all genes in the presence of DMSO or SAHA. *B*, average ChIP-Seq profiles of highly induced and repressed genes in the presence of SAHA.

TABLE 1
Genes highly induced (3 S.D.) by SAHA in MC3T3 sc4 cells

Gene symbol	-fold change	Gene symbol	-fold change	Gene symbol	-fold change
Pkp2	7.5	*Atf3*	2.7	*Ibrdc3*	2.3
Mknk2	5.8	*Ptpn1*	2.7	*Sipa1l2*	2.3
Dyrk3	5.8	*Pgpep1*	2.7	*Ccrn4l*	2.3
Nuak2	5.6	*Arid5a*	2.7	*Cry2*	2.3
5730593F17Rik	5.3	*C630025L14*	2.7	*Spsb1*	2.3
Hist1h1c	5.2	*Dusp14*	2.6	*2810029C07Rik*	2.3
9530053J19Rik	5.1	*Fbxo33*	2.6	*Mfsd7b*	2.3
Slc9a3r1	4.6	*E130216C05Rik*	2.6	*Nfkbie*	2.3
Id1	4.0	*C2cd2l*	2.6	*Atg12*	2.3
Rbm38	3.9	*9930031P18Rik*	2.6	*BC022687*	2.3
1110003O08Rik	3.7	*C130057N11Rik*	2.6	*Phtf2*	2.3
scl0001533.1_63	3.5	*Napepld*	2.6	*Rab3il1*	2.3
6430548M08Rik	3.4	*Pdxp*	2.6	*Csrnp2*	2.3
Rassf5	3.4	*Egr1*	2.6	*Cnp1*	2.3
Nfkbiz	3.4	*Plekho2*	2.6	*LOC100047260*	2.3
Rab3ip	3.4	*AB112350*	2.6	*Micall2*	2.3
Pnpla2	3.3	*Nup43*	2.5	*2610024G14Rik*	2.3
Nr6a1	3.3	*Dos*	2.5	*Ccdc85b*	2.2
Axud1	3.2	*H1f0*	2.5	*Cep152*	2.2
Vps37b	3.2	*Hes1*	2.5	*AI850995*	2.2
Bcl2l11	3.2	*Il17rd*	2.5	*Arhgap29*	2.2
Trp53bp2	3.2	*Usp2*	2.5	*8430427H17Rik*	2.2
scl0001379.1_70	3.2	*Por*	2.5	*Gch1*	2.2
1200012P04Rik	3.1	*Baiap2*	2.5	*Mast3*	2.2
Fbxo31	3.1	*LOC100044177*	2.5	*Ulk1*	2.2
Insl6	3.0	*2410187C16Rik*	2.5	*Usp28*	2.2
Mcam	3.0	*Ptges*	2.5	*Arfl4*	2.2
Sgtb	3.0	*Plcd3*	2.5	*Socs3*	2.2
Errfi1	3.0	*LOC100047651*	2.4	*Jund1*	2.2
Itpk1	2.9	*Daam1*	2.4	*A430083I17Rik*	2.2
9430023L20Rik	2.9	*Ehd4*	2.4	*4930431B09Rik*	2.2
LOC240672	2.9	*Ppargc1b*	2.4	*Fosb*	2.2
LOC100045343	2.9	*C130008L17Rik*	2.4	*LOC100045644*	2.2
Zswim6	2.9	*Camkk1*	2.4	*Ifrg15*	2.2
1110008J03Rik	2.8	*Mettl11a*	2.4	*Pik3cb*	2.2
Notch1	2.8	*4732473B16Rik*	2.4	*Slc24a6*	2.2
Egr2	2.8	*Cbx2*	2.4	*Kin*	2.2
D16H22S680E	2.8	*Cdc42ep2*	2.4	*Ctr9*	2.2
Sox11	2.8	*Rgs4*	2.4	*Stk38l*	2.1
D15Wsu169e	2.8	*2010004M13Rik*	2.4	*Lrig1*	2.1
Atp10d	2.8	*Fos*	2.3	*Pim3*	2.1
1700003E16Rik	2.7	*Obfc2a*	2.3	*Mafk*	2.1
BC046404	2.7				

GGGACGTGGTGTC (forward) and 5′-CCAGGGCTTCACGGCTGCTC (reverse).

RESULTS

SAHA Enhances Osteoblast Differentiation and Induces Histone Acetylation in Osteoblasts—We previously showed that several HDIs (trichostatin A, valproate, and sodium butyrate) promote matrix calcification of MC3T3-E1 calvarial osteoblasts (12). To determine the effects of SAHA on the differentiation of a rapidly mineralizing subclone of MC3T3 cells (sc4), we added SAHA (10 μM) or vehicle (DMSO) to osteogenic cultures on days 4–7 of a 26-day period. Consistent with previous results, SAHA enhanced matrix calcification of MC3T3 sc4 cells (Fig. 1*A*). In time course experiments, we found that SAHA induced hyperacetylation of histones H3 and H4 within 3 h (Fig. 1*B*). Comparable conditions were subsequently used in ChIP-Seq and gene expression microarray studies.

Validation of ChIP Procedure—ChIP assays were performed with control IgG or an anti-acetylated H4 antibody that is ChIP-certified (27). The immunoprecipitation reactions were confirmed by Western blot analysis (Fig. 2*A*). Basal acetylation of H4 was enhanced by SAHA (*I* (input) *lanes*), and more acetylated H4 was precipitated by the anti-H4 antibody from SAHA-treated cells than from vehicle-treated control cells. The non-specific IgG did not bind acetylated H4. These data indicate that the anti-H4 antibody selectively and efficiently precipitates acetylated H4.

The specificity of our ChIP procedure for detection of acetylated H4 on distinct genes was evaluated with primers flanking the *Axin2* promoter. We assessed the acetylation status of acetylated H4 on this DNA region in the presence of SAHA or vehicle (DMSO) (28). Axin2 is a scaffold protein that suppresses canonical Wnt signaling by facilitating the degradation of β-catenin (29). We recently showed that HDAC3 suppresses Axin2 transcription and that Axin2 is regulated by Runx2 in osteoblasts (28). Basal acetylated H4 was detected on the *Axin2* promoter in control cells treated with vehicle, but it was >10-fold higher in SAHA treated cells (Fig. 2*B*). The control IgG antibody did not bind the *Axin2* promoter under either condition. These data demonstrate that SAHA induces H4 acetylation of the *Axin2* promoter, thus prevalidating our ChIP procedures for whole genome sequencing.

SAHA Induces Genome-wide H4 Acetylation—Sequencing libraries were prepared with our ChIP DNA for massively parallel high-throughput sequencing. Genome-wide H4 acetylation patterns were generated and modeled with CEAS software (Fig. 3*A*). H4 acetylation profiles for multiple genes were aver-

TABLE 2
Genes highly suppressed (3 S.D.) by SAHA in MC3T3 sc4 cells

Gene symbol	-fold change	Gene symbol	-fold change	Gene symbol	-fold change
Trib3	−5.3	*Alx4*	−2.6	*0610038D11Rik*	−2.3
Fgf7	−4.9	*Taf9b*	−2.5	*Tmem39a*	−2.3
Suv420h1	−4.8	*Zbtb45*	−2.5	*C030013F01Rik*	−2.3
LOC100044776	−4.8	*Gmeb2*	−2.5	*Kif2c*	−2.3
Herpud1	−4.2	*Nr1h4*	−2.5	*Kbtbd2*	−2.3
Rabl3	−4.1	*Zfp608*	−2.5	*BC002230*	−2.3
Sp7	−3.9	*Atxn7l2*	−2.5	*Dlx1*	−2.3
E130306D19Rik	−3.6	*Dtwd2*	−2.5	*Pcgf1*	−2.3
Chac1	−3.5	*1810063B07Rik*	−2.5	*Elac1*	−2.3
Qrsl1	−3.4	*Kctd15*	−2.5	*Syde1*	−2.3
4930563B10Rik	−3.4	*Tmem68*	−2.5	*Zfp551*	−2.3
D830041I17Rik	−3.4	*Pop7*	−2.5	*Gsc*	−2.3
Tnfrsf11b	−3.4	*Pprc1*	−2.4	*Neu2*	−2.3
1700030K09Rik	−3.4	*Prkcbp1*	−2.4	*Rasl11a*	−2.2
Has2	−3.3	*BC057552*	−2.4	*4930445K14Rik*	−2.2
Zfx	−3.2	*Six5*	−2.4	*Spag7*	−2.2
Pus7l	−3.2	*6530404N21Rik*	−2.4	*Cox10*	−2.2
Yeats4	−3.1	*Irx3*	−2.4	*Asxl1*	−2.2
Hmgb2l1	−3.1	*Aspm*	−2.4	*Hexim2*	−2.2
Mrgprf	−3.1	*9130024F11Rik*	−2.4	*Cox15*	−2.2
Dnm3os	−3.0	*Tada1l*	−2.4	*Vgll3*	−2.2
Gbl	−3.0	*Ccnb1*	−2.4	*Kctd6*	−2.2
Refbp2	−3.0	*Gm962*	−2.4	*Ndufaf1*	−2.2
Arrdc3	−3.0	*Pygo1*	−2.4	*Pus3*	−2.2
Nkd2	−3.0	*Ctcf*	−2.4	*Rpp38*	−2.2
A230051G13Rik	−3.0	*Adamts4*	−2.4	*Zfp532*	−2.2
Fiz1	−2.9	*Axin2*	−2.4	*4930577N17Rik*	−2.2
Fst	−2.9	*Xbp1*	−2.4	*1810009O10Rik*	−2.2
Jmjd5	−2.8	*Gper*	−2.4	*BB146404*	−2.2
Zfp653	−2.8	*Rabif*	−2.3	*Zfp746*	−2.2
Ly96	−2.8	*Plk1*	−2.3	*Nfatc4*	−2.2
Sertad4	−2.8	*Tmem103*	−2.3	*Troap*	−2.2
Slc2a10	−2.8	*Thtpa*	−2.3	*Sirt1*	−2.2
Fzd1	−2.7	*Hmgb2*	−2.3	*2310040B03Rik*	−2.2
2010321M09Rik	−2.7	*A430107N12Rik*	−2.3	*Nek3*	−2.2
A130047F11Rik	−2.7	*Cc2d2a*	−2.3	*9430038I01Rik*	−2.2
D530007E13Rik	−2.7	*2310039E09Rik*	−2.3	*Rg9mtd2*	−2.2
Txnl4b	−2.7	*2610524B01Rik*	−2.3	*1200015N20Rik*	−2.2
Trps1	−2.7	*D830050J10Rik*	−2.3	*Commd7*	−2.2
6430706D22Rik	−2.6	*Znrd1*	−2.3	*Fam13c*	−2.1
Tcfap2b	−2.6	*BC067068*	−2.3	*Gpr23*	−2.1
Tmem185b	−2.6	*Msrb2*	−2.3	*Inhba*	−2.1
2010320M18Rik	−2.6	Map3k7ip1	−2.3	*LOC100048696*	−2.1
Ccdc94	−2.6				

aged and presented as a metagene, which is the average gene profile where genes are normalized to the same length. This analysis revealed that SAHA generally increased acetylated H4 downstream of the transcriptional start site (TSS), including exons, introns and the transcriptional termination site. Strikingly, the levels of acetylated H4 were lower at the TSS in SAHA-treated cells. Reduction in acetylated H4 in SAHA-exposed cells occurred within 500 bp upstream and downstream of TSS. This reduction in H4 acetylation occurred in both induced and repressed genes, but it was more profound in genes whose expression was increased by SAHA (Fig. 3*B*). This may be a direct result of fewer nucleosomes at TSSs (30, 31).

Correlation between H4 Acetylation and Gene Expression—To correlate H4 acetylation patterns with modulations in gene expression, we performed gene expression analysis using microarrays with mRNA from MC3T3 sc4 cells treated with SAHA or its DMSO solvent. SAHA significantly increased the expression levels of 127 transcripts (Table 1) and suppressed expression of 130 genes (Table 2) by >2-fold within 3 S.D. of the mean. CEAS analysis of these differentially regulated groups showed that SAHA broadly increased H4 acetylation in both up- and down-regulated genes compared with the entire gene set (Fig. 3*B*). Genes of transcripts induced by SAHA had greater levels of acetylated H4 in introns, exons, and the transcriptional termination site than down-regulated genes. Profiles for three of the most up-regulated genes (*Pkp2*, +7.49-fold; *Mknk2*, +5.84-fold; and *Slc9a3r1*, +4.69-fold) and two of the most suppressed genes (*Trib3*, −5.31-fold; and *Herpud1*, −4.23-fold) are shown in Fig. 4. The results demonstrate that SAHA-induced H4 hyperacetylation is generally greater in highly expressed genes.

Less straightforward is the observation that genes encoding transcripts suppressed by SAHA also had more acetylated H4 compared with the entire set of genes whose expression was not affected by SAHA. This suggests that SAHA may enforce an acetylated state, but transcriptional suppressors are dominant in certain contexts. We also found that H4 was less acetylated within the initial 500 bp upstream of the TSSs of highly induced genes compared with genes suppressed by SAHA (Fig. 3*B*). This result is most easily explained by increased density of nucleosomes (and thus the efficiency of detecting acetylated H4) on suppressed genes.

SAHA Interferes with Insulin Signaling—To identify pathways that are affected by SAHA in MC3T3 sc4 cells, the microarray gene expression dataset was subjected to pathway analysis using DAVID (database for annotation, visualization

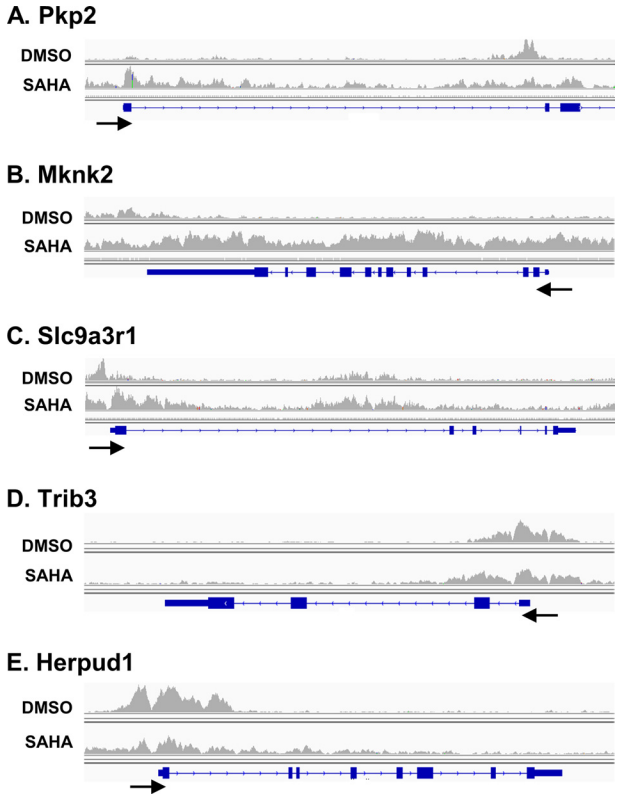

FIGURE 4. **ChIP-Seq profiles of genes differentially expressed in the presence of SAHA.** MC3T3 sc4 cells were differentiated in osteogenic medium for 4 days and treated with DMSO or SAHA (20 μM) for 2 h before the ChIP-Seq assay was performed with anti-acetylated H4 and control IgG antibodies. *A*, *Pkp2* (induced 7.49-fold by SAHA). *B*, *Mknk2* (induced 5.84-fold by SAHA). *C*, *Slc9a3r1* (induced 4.6-fold by SAHA). *D*, *Trib3* (suppressed 5.31-fold by SAHA). *E*, *Herpud1* (suppressed 4.23-fold by SAHA). *Arrows* indicate the orientation and TSS.

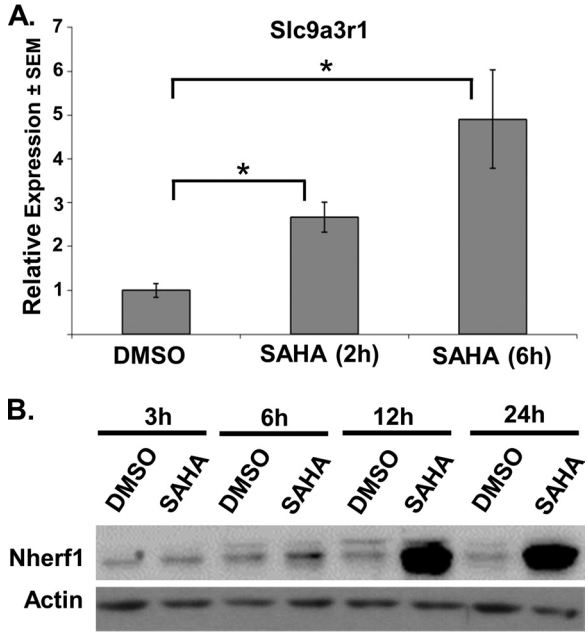

FIGURE 5. **SAHA induces *Slc9a3r1* mRNA and protein (Nherf1) levels.** *A*, qPCR analysis of MC3T3 sc4 cells treated with DMSO or SAHA. MC3T3 sc4 cells were differentiated in osteogenic medium for 4 days and then treated with DMSO or SAHA (20 μM) for 2 and 6 h before mRNA was isolated and qPCR was performed. Data are mean ± S.E. ($n = 4$). *, $p < 0.05$ *versus* vehicle (DMSO) treatment. *B*, Western blotting of MC3T3 sc4 cells treated with DMSO and SAHA. Subconfluent MC3T3 sc4 cells were treated with DMSO and 10 μM SAHA for 3, 6, 12, and 24 h.

and integrated discovery) analysis software (32, 33). This bioinformatics analysis indicated that the insulin signaling pathway was altered by SAHA in MC3T3 sc4 osteoblasts. Five highly up-regulated genes (*Mknk2*, +5.84-fold; *Slc9a3r1*, +4.59-fold; *Ptpn1*, +2.71-fold; *Socs3*, +2.19-fold; and *Pik3cb*, +2.16-fold) play a critical role in insulin signaling.

Slc9a3r1 stood out among these because we previously found it to be one of the most highly and consistently induced genes in MC3T3 cells treated with other HDIs (20). Increases in *Slc9a3r1*/Nherf1 expression in response to SAHA were confirmed by qPCR (Fig. 5*A*) and Western blotting (Fig. 5*B*). Nherf1 (Na^+/H^+ exchanger regulatory factor 1), which is the protein encoded by the *Slc9a3r1* gene, is an adaptor protein that facilitates the interaction of Akt with protein-tyrosine phosphatases Phlpp and Pten (34).

To determine the effects of SAHA on the insulin/Akt signaling pathway, subconfluent MC3T3 sc4 cells were treated with SAHA for 24 h, and Western blotting was performed on cell lysates with antibodies for insulin signaling intermediates (Fig. 6*A*). Low concentrations of SAHA (1 μM) did not affect the phosphorylation status of key intermediates of the insulin pathway. In contrast, higher SAHA concentrations (*e.g.* 10 μM) profoundly reduced the phosphorylation of insulin receptor β, the principal initiator of insulin signaling. Phosphorylation of Akt, a key downstream facilitator of insulin signaling, was reduced by 76% (Fig. 6*B*). FoxO1 is an Akt substrate that is stabilized by phosphorylation. In accordance with reduced Akt activation, SAHA decreased FoxO1 phosphorylation, which resulted in higher total FoxO1 protein levels after 24 h (Fig. 6, *A* and *B*). Insulin reversed the effects of SAHA on Akt phosphorylation after just 5 min of treatment (Fig. 6, *C* and *D*) but did not affect FoxO1 in this short period of time. These results indicate that the proximal insulin signaling pathway is not permanently or dominantly suppressed by SAHA. Both insulin and SAHA induced osteoblast differentiation *in vitro* (Fig. 6, *E* and *F*); however, there was no enhancement of SAHA-induced calcification with insulin. Together, these data indicate that SAHA stimulates osteoblast differentiation despite the underphosphorylation and suppressed activity of crucial mediators of the anabolic insulin/Akt signaling pathway.

DISCUSSION

Bones can regenerate an optimally mineralized matrix capable of coping with the range of mechanical forces normally experienced in daily life. However, the ability to form new bone capable of load bearing diminishes with age. Moreover, there is a need to optimize bone tissue-engineering strategies for the treatment of non-union fractures and critical size defects. Numerous laboratories have reported that HDIs enhance osteoblast differentiation *in vitro* (11–15, 35–37). In this study, we characterized epigenetic events that occur in SAHA-treated osteoblasts to understand the pathways that control osteoblast differentiation. Our data show that SAHA broadly induces H4 acetylation despite altering the phosphorylation of insulin signaling mediators.

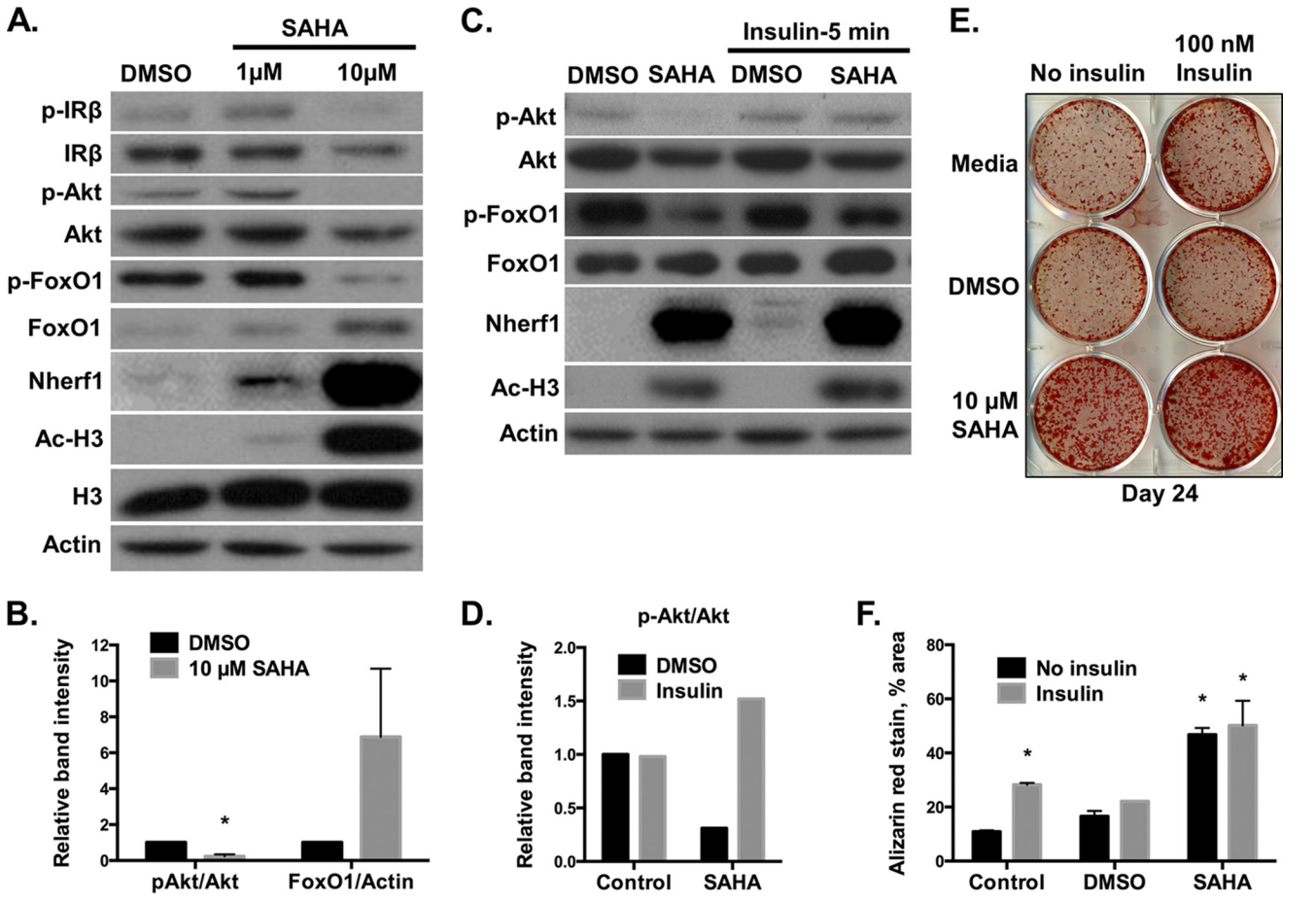

FIGURE 6. **SAHA disrupts insulin signaling in osteoblasts.** *A*, subconfluent MC3T3 sc4 cells were treated with DMSO and SAHA (1 and 10 μM) for 24 h. Western blotting was performed with the indicated antibodies. *p-IRβ*, phospho-insulin receptor β; *Ac-H3*, acetylated H3. *B*, mean relative intensities (±S.E.) of phospho-Akt/Akt and FoxO1/actin bands from three independent experiments ($n = 3$). *, $p < 0.05$. *C*, the effects of SAHA on insulin signaling pathway are restored by insulin addition. Subconfluent MC3T3 sc4 cells were treated with DMSO and 10 μM SAHA for 24 h. 100 nM insulin was added to the cells for 5 min. *D*, relative intensities of phospho-Akt/Akt bands from *C*. *E*, Alizarin red stains of MC3T3 sc4 cells in osteogenic medium for 24 days. DMSO and SAHA (10 μM) were added on day 4 and were removed on day 7 of differentiation, whereas insulin (100 nM) was added daily on days 4–6. *F*, percent areas (±S.E.) of Alizarin red staining in MC3T3 sc4 cells treated with insulin and/or SAHA ($n = 3$). *, $p < 0.05$ relative to control samples.

Previous work demonstrated that HDIs induce matrix mineralization *in vitro*. Indeed, we confirmed that SAHA stimulated matrix calcification and terminal differentiation of MC3T3 sc4 osteoblasts. Similar to previous studies, genes were both induced and suppressed by SAHA (38–40). Gene transcription is believed to be largely due to direct effects on chromatin leading to enhanced histone acetylation; however, indirect effects are also possible. Gene repression is likely to be due entirely to secondary or tertiary events related to SAHA-induced transcription or other mechanisms. For example, SAHA-induced genes may encode transcriptional repressors that could locally reverse the effects of SAHA on specific groups of genes.

ChIP-Seq analysis revealed that SAHA induced genome-wide H4 acetylation. Interestingly, both up- and down-regulated genes broadly exhibited H4 acetylation upon SAHA exposure. The main exception to this global observation was the general decrease in the level of H4 acetylation within 500 bp upstream of the TSS. SAHA-induced H4 acetylation was lower in highly induced genes compared with suppressed genes. Similar observations were made in human HepG2 cells treated with butyrate, a natural HDI (41). The most likely explanation for this result is that nucleosomes are modified, less tightly associated, and/or absent in chromatin of genes that are actively transcribed (30, 31). The resulting reduction in total histone would reduce the efficiency of ChIP.

Pathway analysis indicated that SAHA altered the expression of insulin signaling modulators, including *Slc9a3r1*/Nherf1. We previously reported that *Slc9a3r1*/Nherf1 is highly induced in MC3T3-E1 cells following treatment with three other HDIs (trichostatin A, MS-275, and valproate) (20), making it the most consistently induced gene in response to HDIs in osteoblasts. Nherf1 is an adaptor protein that facilitates the interaction of Akt with protein-tyrosine phosphatases Phlpp and Pten to suppress insulin signaling (34). This prompted us to examine insulin/Akt signaling in SAHA-exposed osteoblasts. We found that SAHA decreased immediate signaling through the insulin/Akt pathway. This was demonstrated by decreased phosphorylation of insulin receptor β, Akt, and ultimately FoxO1. Similar results were observed with another HDI, LBH-589 (data not shown). Insulin was capable of inducing Akt and FoxO1 phosphorylation in the presence or absence of SAHA, but it did not decrease Nherf1 levels in SAHA-treated cells. These results suggest that Nherf1, although highly induced by SAHA and important for

osteogenesis (42), may not be an important factor controlling insulin signaling in osteoblasts. Nherf1 also scaffolds protein complexes that associate with the parathyroid hormone receptor and Na^+/H^+ exchangers (43, 44) and may contribute to the increased osteogenesis observed in SAHA-treated cultures.

The mechanism(s) responsible for reduced insulin/Akt signaling after SAHA treatment is not clear at this time. It may be that higher amounts of Nherf1 facilitate the association of phosphatases with the insulin receptor. We recently showed that HDAC3 deletion and SAHA exposure increased expression of the Phlpp1 phosphatase in chondrocytes (45); however, we have not observed changes in Phlpp1 levels in SAHA-treated or HDAC3-deficient osteoblasts. Thus, alterations in Akt signaling after SAHA treatment occur by different mechanisms in osteoblasts than in chondrocytes.

Although further work is necessary to elucidate the connection between histone acetylation status and insulin signaling, this study clearly demonstrates the potential of epigenomic analyses in understanding osteoblast biology. In addition to providing new insights into pathways that control osteoblast function, epigenomic studies provide detailed information on the chromatin structure of osteoblast-specific genes. Numerous HDACs are expressed and active in osteoblasts (8). They associate with transcription factors, such as Runx2, to regulate gene expression. The ChIP-Seq data reported here offer regulatory information on gene locations that can be hyperacetylated and thus pinpoint important osteoblast-specific control regions.

In conclusion, this is the first report to document genome-wide H4 acetylation patterns in osteoblasts treated with an HDI. The enhanced H4 acetylation is characterized by altered expression of osteoblast gene regulatory programs. The insulin signaling pathway was identified as a major pathway controlled by SAHA that may be fundamentally connected to the mineralization-promoting anabolic functions of SAHA in cultured osteoblasts.

REFERENCES

1. Gibney, E. R., and Nolan, C. M. (2010) Epigenetics and gene expression. *Heredity* **105,** 4–13
2. Grunstein, M. (1997) Histone acetylation in chromatin structure and transcription. *Nature* **389,** 349–352
3. Peterson, C. L., and Laniel, M. A. (2004) Histones and histone modifications. *Curr. Biol.* **14,** R546–R551
4. Gryder, B. E., Sodji, Q. H., and Oyelere, A. K. (2012) Targeted cancer therapy: giving histone deacetylase inhibitors all they need to succeed. *Future Med. Chem.* **4,** 505–524
5. Kim, H. J., and Bae, S. C. (2011) Histone deacetylase inhibitors: molecular mechanisms of action and clinical trials as anti-cancer drugs. *Am. J. Transl. Res.* **3,** 166–179
6. Wightman, F., Ellenberg, P., Churchill, M., and Lewin, S. R. (2012) HDAC inhibitors in HIV. *Immunol. Cell Biol.* **90,** 47–54
7. Hutt, D. M., Herman, D., Rodrigues, A. P., Noel, S., Pilewski, J. M., Matteson, J., Hoch, B., Kellner, W., Kelly, J. W., Schmidt, A., Thomas, P. J., Matsumura, Y., Skach, W. R., Gentzsch, M., Riordan, J. R., Sorscher, E. J., Okiyoneda, T., Yates, J. R., 3rd, Lukacs, G. L., Frizzell, R. A., Manning, G., Gottesfeld, J. M., and Balch, W. E. (2010) Reduced histone deacetylase 7 activity restores function to misfolded CFTR in cystic fibrosis. *Nat. Chem. Biol.* **6,** 25–33
8. McGee-Lawrence, M. E., and Westendorf, J. J. (2011) Histone deacetylases in skeletal development and bone mass maintenance. *Gene* **474,** 1–11
9. Rahman, M. M., Kukita, A., Kukita, T., Shobuike, T., Nakamura, T., and Kohashi, O. (2003) Two histone deacetylase inhibitors, trichostatin A and sodium butyrate, suppress differentiation into osteoclasts but not into macrophages. *Blood* **101,** 3451–3459
10. Yi, T., Baek, J. H., Kim, H. J., Choi, M. H., Seo, S. B., Ryoo, H. M., Kim, G. S., and Woo, K. M. (2007) Trichostatin A-mediated upregulation of $p21^{WAF1}$ contributes to osteoclast apoptosis. *Exp. Mol. Med.* **39,** 213–221
11. Iwami, K., and Moriyama, T. (1993) Effects of short chain fatty acid, sodium butyrate, on osteoblastic cells and osteoclastic cells. *Int. J. Biochem.* **25,** 1631–1635
12. Schroeder, T. M., and Westendorf, J. J. (2005) Histone deacetylase inhibitors promote osteoblast maturation. *J. Bone Miner. Res.* **20,** 2254–2263
13. Lee, S., Park, J. R., Seo, M. S., Roh, K. H., Park, S. B., Hwang, J. W., Sun, B., Seo, K., Lee, Y. S., Kang, S. K., Jung, J. W., and Kang, K. S. (2009) Histone deacetylase inhibitors decrease proliferation potential and multilineage differentiation capability of human mesenchymal stem cells. *Cell Prolif.* **42,** 711–720
14. Di Bernardo, G., Squillaro, T., Dell'Aversana, C., Miceli, M., Cipollaro, M., Cascino, A., Altucci, L., and Galderisi, U. (2009) Histone deacetylase inhibitors promote apoptosis and senescence in human mesenchymal stem cells. *Stem Cells Dev.* **18,** 573–581
15. Haberland, M., Carrer, M., Mokalled, M. H., Montgomery, R. L., and Olson, E. N. (2010) Redundant control of adipogenesis by histone deacetylases 1 and 2. *J. Biol. Chem.* **285,** 14663–14670
16. Lee, H. W., Suh, J. H., Kim, A. Y., Lee, Y. S., Park, S. Y., and Kim, J. B. (2006) Histone deacetylase 1-mediated histone modification regulates osteoblast differentiation. *Mol. Endocrinol.* **20,** 2432–2443
17. Schroeder, T. M., Kahler, R. A., Li, X., and Westendorf, J. J. (2004) Histone deacetylase 3 interacts with Runx2 to repress the osteocalcin promoter and regulate osteoblast differentiation. *J. Biol. Chem.* **279,** 41998–42007
18. Westendorf, J. J., Zaidi, S. K., Cascino, J. E., Kahler, R., van Wijnen, A. J., Lian, J. B., Yoshida, M., Stein, G. S., and Li, X. (2002) Runx2 (Cbfa1, AML-3) interacts with histone deacetylase 6 and represses the $p21^{CIP1/WAF1}$ promoter. *Mol. Cell. Biol.* **22,** 7982–7992
19. Jensen, E. D., Schroeder, T. M., Bailey, J., Gopalakrishnan, R., and Westendorf, J. J. (2008) Histone deacetylase 7 associates with Runx2 and represses its activity during osteoblast maturation in a deacetylation-independent manner. *J. Bone Miner. Res.* **23,** 361–372
20. Schroeder, T. M., Nair, A. K., Staggs, R., Lamblin, A. F., and Westendorf, J. J. (2007) Gene profile analysis of osteoblast genes differentially regulated by histone deacetylase inhibitors. *BMC Genomics* **8,** 362
21. Wang, D., Christensen, K., Chawla, K., Xiao, G., Krebsbach, P. H., and Franceschi, R. T. (1999) Isolation and characterization of MC3T3-E1 preosteoblast subclones with distinct *in vitro* and *in vivo* differentiation/mineralization potential. *J. Bone Miner. Res.* **14,** 893–903
22. Li, H., and Durbin, R. (2009) Fast and accurate short read alignment with Burrows-Wheeler transform. *Bioinformatics* **25,** 1754–1760
23. Zhang, Y., Liu, T., Meyer, C. A., Eeckhoute, J., Johnson, D. S., Bernstein, B. E., Nusbaum, C., Myers, R. M., Brown, M., Li, W., and Liu, X. S. (2008) Model-based analysis of ChIP-Seq (MACS). *Genome Biol.* **9,** R137
24. Ji, X., Li, W., Song, J., Wei, L., and Liu, X. S. (2006) CEAS: *cis*-regulatory element annotation system. *Nucleic Acids Res.* **34,** W551–W554
25. Shin, H., Liu, T., Manrai, A. K., and Liu, X. S. (2009) CEAS: *cis*-regulatory element annotation system. *Bioinformatics* **25,** 2605–2606
26. Ballman, K. V., Grill, D. E., Oberg, A. L., and Therneau, T. M. (2004) Faster cyclic loess: normalizing RNA arrays via linear models. *Bioinformatics* **20,** 2778–2786
27. Alberts, A. S., Geneste, O., and Treisman, R. (1998) Activation of SRF-regulated chromosomal templates by Rho-family GTPases requires a signal that also induces H4 hyperacetylation. *Cell* **92,** 475–487
28. McGee-Lawrence, M. E., Li, X., Bledsoe, K. L., Wu, H., Hawse, J. R., Subramaniam, M., Razidlo, D. F., Stensgard, B. A., Stein, G. S., van Wijnen, A. J., Lian, J. B., Hsu, W., and Westendorf, J. J. (2013) Runx2 protein represses Axin2 expression in osteoblasts and is required for craniosynostosis in *Axin2*-deficient mice. *J. Biol. Chem.* **288,** 5291–5302
29. Westendorf, J. J., Kahler, R. A., and Schroeder, T. M. (2004) Wnt signaling in osteoblasts and bone diseases. *Gene* **341,** 19–39
30. Kaplan, N., Moore, I. K., Fondufe-Mittendorf, Y., Gossett, A. J., Tillo, D., Field, Y., LeProust, E. M., Hughes, T. R., Lieb, J. D., Widom, J., and Segal, E.

(2009) The DNA-encoded nucleosome organization of a eukaryotic genome. *Nature* **458,** 362–366
31. Sadeh, R., and Allis, C. D. (2011) Genome-wide "re"-modeling of nucleosome positions. *Cell* **147,** 263–266
32. Huang, D. W., Sherman, B. T., and Lempicki, R. A. (2009) Systematic and integrative analysis of large gene lists using DAVID bioinformatics resources. *Nat. Protoc.* **4,** 44–57
33. Huang, D., W., Sherman, B. T., and Lempicki, R. A. (2009) Bioinformatics enrichment tools: paths toward the comprehensive functional analysis of large gene lists. *Nucleic Acids Res.* **37,** 1–13
34. Molina, J. R., Agarwal, N. K., Morales, F. C., Hayashi, Y., Aldape, K. D., Cote, G., and Georgescu, M. M. (2012) PTEN, NHERF1 and PHLPP form a tumor suppressor network that is disabled in glioblastoma. *Oncogene* **31,** 1264–1274
35. Maroni, P., Brini, A. T., Arrigoni, E., de Girolamo, L., Niada, S., Matteucci, E., Bendinelli, P., and Desiderio, M. A. (2012) Chemical and genetic blockade of HDACs enhances osteogenic differentiation of human adipose tissue-derived stem cells by oppositely affecting osteogenic and adipogenic transcription factors. *Biochem. Biophys. Res. Commun.* **428,** 271–277
36. Hu, X., Zhang, X., Dai, L., Zhu, J., Jia, Z., Wang, W., Zhou, C., and Ao, Y. (2013) Histone deacetylase inhibitor trichostatin A promotes the osteogenic differentiation of rat adipose-derived stem cells by altering the epigenetic modifications on *Runx2* promoter in a BMP signaling-dependent manner. *Stem Cells Dev.* **22,** 248–255
37. Kim, H. N., Lee, J. H., Bae, S. C., Ryoo, H. M., Kim, H. H., Ha, H., and Lee, Z. H. (2011) Histone deacetylase inhibitor MS-275 stimulates bone formation in part by enhancing Dhx36-mediated TNAP transcription. *J. Bone Miner. Res.* **26,** 2161–2173
38. Marrocco, D. L., Tilley, W. D., Bianco-Miotto, T., Evdokiou, A., Scher, H. I., Rifkind, R. A., Marks, P. A., Richon, V. M., and Butler, L. M. (2007) Suberoylanilide hydroxamic acid (vorinostat) represses androgen receptor expression and acts synergistically with an androgen receptor antagonist to inhibit prostate cancer cell proliferation. *Mol. Cancer Ther.* **6,** 51–60
39. LaBonte, M. J., Wilson, P. M., Fazzone, W., Groshen, S., Lenz, H. J., and Ladner, R. D. (2009) DNA microarray profiling of genes differentially regulated by the histone deacetylase inhibitors vorinostat and LBH589 in colon cancer cell lines. *BMC Med. Genomics* **2,** 67
40. Yin, D., Ong, J. M., Hu, J., Desmond, J. C., Kawamata, N., Konda, B. M., Black, K. L., and Koeffler, H. P. (2007) Suberoylanilide hydroxamic acid, a histone deacetylase inhibitor: effects on gene expression and growth of glioma cells *in vitro* and *in vivo*. *Clin. Cancer Res.* **13,** 1045–1052
41. Rada-Iglesias, A., Enroth, S., Ameur, A., Koch, C. M., Clelland, G. K., Respuela-Alonso, P., Wilcox, S., Dovey, O. M., Ellis, P. D., Langford, C. F., Dunham, I., Komorowski, J., and Wadelius, C. (2007) Butyrate mediates decrease of histone acetylation centered on transcription start sites and down-regulation of associated genes. *Genome Res.* **17,** 708–719
42. Liu, L., Alonso, V., Guo, L., Tourkova, I., Henderson, S. E., Almarza, A. J., Friedman, P. A., and Blair, H. C. (2012) Na^+/H^+ exchanger regulatory factor 1 (NHERF1) directly regulates osteogenesis. *J. Biol. Chem.* **287,** 43312–43321
43. Wang, B., Bisello, A., Yang, Y., Romero, G. G., and Friedman, P. A. (2007) NHERF1 regulates parathyroid hormone receptor membrane retention without affecting recycling. *J. Biol. Chem.* **282,** 36214–36222
44. Wang, B., Yang, Y., Abou-Samra, A. B., and Friedman, P. A. (2009) NHERF1 regulates parathyroid hormone receptor desensitization: interference with β-arrestin binding. *Mol. Pharmacol.* **75,** 1189–1197
45. Bradley, E. W., Carpio, L. R., and Westendorf, J. J. (2013) Histone deacetylase 3 suppression increases PH domain and leucine-rich repeat phosphatase (Phlpp)1 expression in chondrocytes to suppress Akt signaling and matrix secretion. *J. Biol. Chem.* **288,** 9572–9582